Cell Stem Cell
Article

The Two Active X Chromosomes in Female ESCs Block Exit from the Pluripotent State by Modulating the ESC Signaling Network

Edda G. Schulz,[1,*] Johannes Meisig,[2,3] Tomonori Nakamura,[4,5] Ikuhiro Okamoto,[4,5] Anja Sieber,[2,3] Christel Picard,[1] Maud Borensztein,[1] Mitinori Saitou,[4,5,6,7] Nils Blüthgen,[2,3] and Edith Heard[1,*]
[1]Mammalian Developmental Epigenetics Group, Institut Curie, CNRS UMR 3215, INSERM U934, Paris 75248, France
[2]Institute of Pathology, Charité-Universitätsmedizin, 10117 Berlin, Germany
[3]Integrative Research Institute for the Life Sciences and Institute for Theoretical Biology, Humboldt Universität, 10115 Berlin, Germany
[4]Department of Anatomy and Cell Biology, Graduate School of Medicine, Kyoto University, Yoshida-Konoe-cho, Sakyo-ku, Kyoto 606-8501, Japan
[5]JST, ERATO, Yoshida-Konoe-cho, Sakyo-ku, Kyoto 606-8501, Japan
[6]Center for iPS Cell Research and Application, Kyoto University, 53 Kawahara-cho, Shogoin Yoshida, Sakyo-ku, Kyoto 606-8507, Japan
[7]Institute for Integrated Cell-Material Sciences, Kyoto University, Yoshida-Ushinomiya-cho, Sakyo-ku, Kyoto 606-8501, Japan
*Correspondence: edda.schulz@curie.fr (E.G.S.), edith.heard@curie.fr (E.H.)
http://dx.doi.org/10.1016/j.stem.2013.11.022

SUMMARY

During early development of female mouse embryos, both X chromosomes are transiently active. X gene dosage is then equalized between the sexes through the process of X chromosome inactivation (XCI). Whether the double dose of X-linked genes in females compared with males leads to sex-specific developmental differences has remained unclear. Using embryonic stem cells with distinct sex chromosome compositions as a model system, we show that two X chromosomes stabilize the naive pluripotent state by inhibiting MAPK and Gsk3 signaling and stimulating the Akt pathway. Since MAPK signaling is required to exit the pluripotent state, differentiation is paused in female cells as long as both X chromosomes are active. By preventing XCI or triggering it precociously, we demonstrate that this differentiation block is released once XX cells have undergone X inactivation. We propose that double X dosage interferes with differentiation, thus ensuring a tight coupling between X chromosome dosage compensation and development.

INTRODUCTION

During early embryogenesis in many mammals, such as mice, rats, and cows, female embryos develop more slowly than males (Mittwoch, 1993). Since no fetal hormones are produced at these stages of embryonic development, the observed developmental sex differences have been attributed to a direct action of sex-linked genes. Genetic dissection using mice with an XO karyotype revealed that the presence of two X chromosomes contributes to the developmental differences by slowing down embryogenesis early after implantation into the uterus (Burgoyne et al., 1995).

In somatic tissues, the difference in X chromosome number between the sexes is compensated for through the process of X chromosome inactivation (XCI), which ensures chromosome-wide gene silencing of one X in all female cells (Augui et al., 2011; Schulz and Heard, 2013). XCI is initiated by upregulation of the noncoding Xist RNA at the future inactive X, which then mediates gene silencing in *cis*. During murine preimplantation development, *Xist* expression is imprinted so that the paternal X is always inactivated. While this imprinted form of XCI is maintained in extraembryonic tissues, the paternal X is reactivated in the inner cell mass (ICM) of the blastocyst, which will give rise to the embryo. Shortly afterward, one randomly chosen X is inactivated at the epiblast stage. Thus, the two X chromosomes in female embryos are both active during a short time window around implantation. Whether (and how) this resulting transient double dose of X-linked genes affects development in a sex-specific manner has remained unclear.

In the mouse, which is the best-studied mammal to date, X inactivation is set up before lineage commitment occurs, at a point when each cell can give rise to all somatic and germline cell types and thus is pluripotent. Tight coupling between XCI and development is thought to be ensured through direct and indirect repression of *Xist* by pluripotency factors such as Oct4, Nanog, and Rex1, so that XCI is only initiated once these factors are downregulated during differentiation (Augui et al., 2011). These regulatory relationships have been studied mostly in female mouse embryonic stem cell (mESC) lines derived from the ICM of the blastocyst, which have two active X chromosomes and undergo random XCI during in vitro differentiation. When induced to differentiate, ESCs exit the so-called ground state of pluripotency, transition through a primed state in which certain pluripotency factors are downregulated and XCI is initiated, and only then adopt a specific cell fate (Nichols and Smith, 2009). The transition to the primed state is strongly dependent on autocrine growth factor Fgf4, which signals via the mitogen-activated protein kinase (MAPK) cascade (Lanner and Rossant, 2010). Through ectopic inhibition of this pathway in combination with a Gsk3 inhibitor ("2i" culture conditions), ESCs can be maintained in a pluripotent ground state (Ying et al., 2008), in contrast

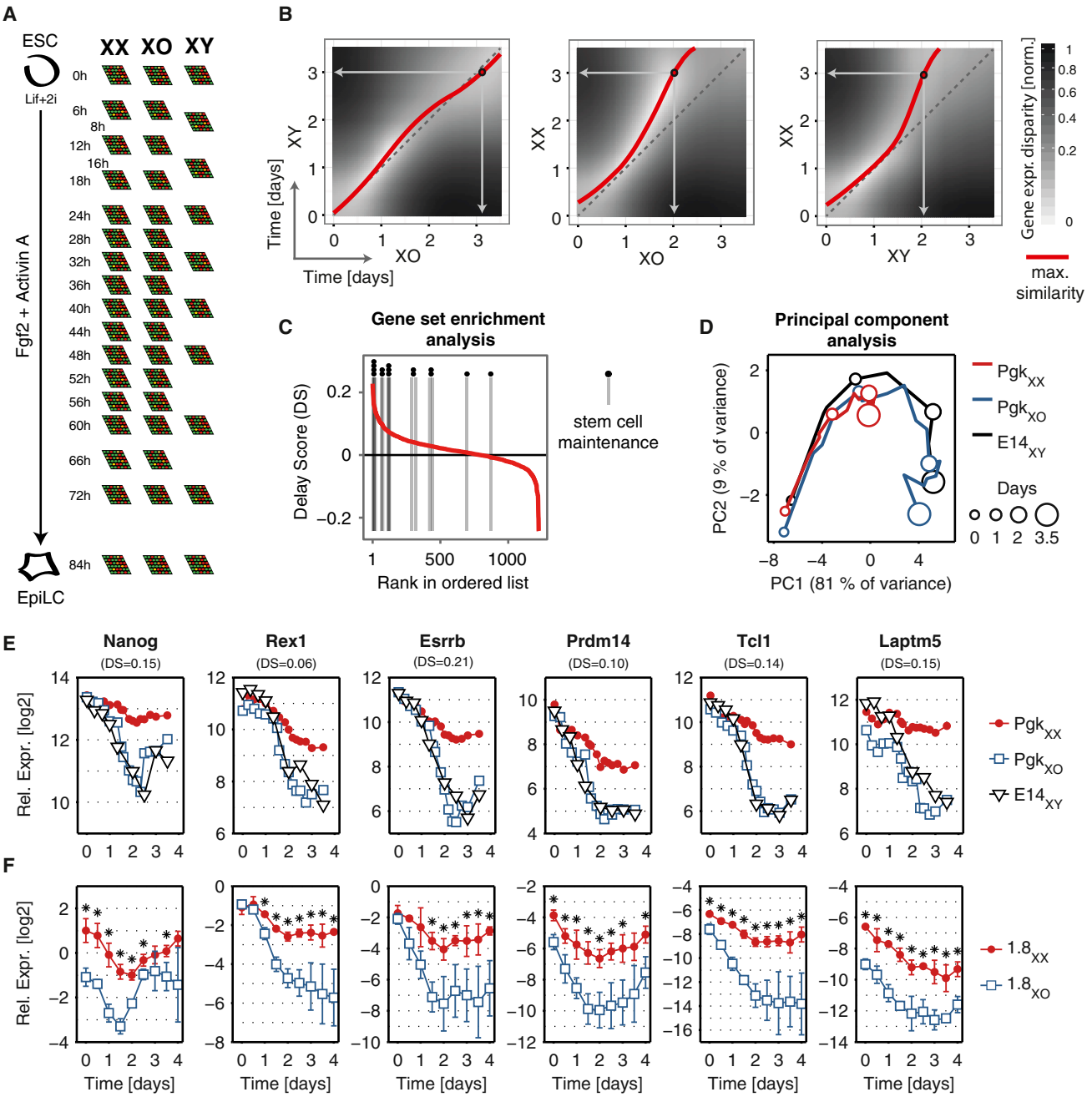

Figure 1. Two X Chromosomes Delay mESC Differentiation

(A) Experimental setup: XX (PGK12.1), XO (derived from PGK12.1), and XY (E14) ESCs, cultured in serum-free medium with 2i and LIF were differentiated into epiblast-like cells (EpiLC) with Fgf2 and Activin A for 3.5 days. At the indicated time points, mRNA levels were assessed genome wide using Affymetrix mouse exon microarrays.

(B) Comparison of gene-expression kinetics among XX, XO, and XY mESCs. Heatmaps show similarity with respect to gene-expression levels between the different cell lines at different time points as measured by the Euclidean distance of all genes that change significantly over time (1,391 genes). Dashed lines indicate the diagonal and red lines indicate the maximal similarity. Arrows are visual guides that link day 3 on the y axis to the most similar time point on the x axis.

(C) GSEA for GO terms in genes that show delayed kinetics in XX cells. For each gene, the delay was quantified as the difference of the mean derivatives in XX and XO cells (red line). "Stem cell maintenance" was significantly enriched (FDR < 0.05) and gray lines with dots indicate the positions of the associated genes. The top ten GO terms are given in Table S1 and a list of delay scores is provided in Table S2.

(D) PCA of genes annotated with the GO term "stem cell maintenance." The first two PCs are plotted; circles represent the day of differentiation as indicated. See Figure S1A and Table S3 for PC loadings.

(legend continued on next page)

to the metastable state found in classical serum-containing medium supplemented with leukemia inhibitory factor (LIF), where cells fluctuate between the ground state and a primed state (Graf and Stadtfeld, 2008). Whereas the MAPK and Gsk3 pathways destabilize the pluripotent state, the Lif/Stat3 and Pi3K/Akt signaling pathways are required to maintain self-renewal and pluripotency (Welham et al., 2011).

In order to investigate the role of X dosage and dosage compensation in ESCs and differentiation as a model for early embryonic development, we performed a genome-wide transcriptome comparison of mESC lines with distinct sex chromosome compositions (XX, XO, and XY). We found that double X chromosome dosage stabilizes the pluripotency network and blocks the exit from the pluripotent state by interfering with the ESC signaling network, thus resulting in delayed differentiation of XX mESCs. We further demonstrate that only after X inactivation has occurred, and only a single dose of X-linked genes remains, can XX cells efficiently downregulate pluripotency factors. We propose that two active X chromosomes arrest differentiation to ensure the coordination of X inactivation and development, so that differentiation is on hold until X dosage compensation has been achieved.

RESULTS

Two Active X Chromosomes Block the Exit from the Pluripotent State

To assess the role of X dosage in early differentiation, we used an in vitro system in which mESCs are differentiated into epiblast-like cells (EpiLC) (Guo et al., 2009). The EpiLC transcriptome has been shown to resemble that of the early epiblast in vivo (Hayashi et al., 2011), which corresponds to the first stage of embryonic development in which X inactivation occurs in mice. We compared the differentiation kinetics (starting from 2i culture conditions, as shown in Ying et al., 2008; see Experimental Procedures) of three mESC lines with distinct sex chromosome compositions: a female XX line (Pgk12.1), an XO subclone of this line that had lost one X (Pgk12.1 E8), and a male XY line from a related genetic background (E14). At multiple time points within the first 3.5 days of differentiation (XCI is initiated between days 1 and 2), we analyzed the transcriptome profiles of these cells using Affymetrix mouse exon arrays (Figure 1A). When we compared the overall transcript dynamics, we found that although the kinetics of the XO and XY cells were similar, the XX line started to lag behind after the first day of differentiation (Figure 1B). Its overall transcript levels started to resemble earlier time points in the XO and XY lines, such that at day 3, XX cells were comparable to the XO and XY lines at day 2 of differentiation (Figure 1B, middle right, arrows). To decipher which processes are delayed in XX cells, we quantified the delay of each gene and performed a gene set enrichment analysis (GSEA) for Gene Ontology (GO) terms (Figure 1C; Tables S1 and S2 available online). The only terms that were significantly enriched among those genes with a strong delay in XX cells (GSEA, false discovery rate [FDR] < 0.05) were "stem cell maintenance" (Figure 1C, gray lines) and "stem cell development," suggesting that the presence of two X chromosomes delays the exit from the stem cell state. We confirmed this interpretation by analyzing the expression profiles of the stem cell maintenance factors through principal component analysis (PCA), which showed that even though all three cell lines followed similar trajectories, the XX line started to be delayed by day 1 and seemed to be almost arrested at day 2 of differentiation (Figures 1D and S1A; Table S3). The transcript abundances of pluripotency factors and other delayed genes were similar in all three cell lines during the first day and then XO and XY cells showed a rapid drop, whereas levels remained much higher in the XX line (see examples in Figure 1E). This delayed downregulation of pluripotency factors was also observed in serum-cultured cells differentiated by LIF withdrawal (Figure S1B) and after adaptation to 2i conditions for more than ten passages (Figure S1C). To confirm that indeed the number of X chromosomes was responsible for the observed delay in differentiation, we tested another XX/XO mESC line pair (1.8XX/XO, identical genetic backgrounds), and once more, upon differentiation, the XX cells downregulated all factors tested with slower kinetics and to a lesser extent than the XO line (Figure 1F). These results show that the observed X chromosome-dependent differentiation arrest is not specific to the mESC line or differentiation system used. Therefore, we conclude that the presence of two X chromosomes delays differentiation of mESCs.

X Dosage Modulates Signaling Pathways in mESCs

When we analyzed the expression kinetics of a panel of pluripotency-associated genes in XX and XO mESCs, we noticed that in serum-containing medium, several genes, including well-known pluripotency factors (but not *Rex1* and *Oct4*), were already increased in XX cells that were still in the undifferentiated state (Figures 2A, S1B, and S2A). Since these expression differences were neutralized in 2i medium (Figure 2B), we hypothesized that the X chromosome number might affect the pluripotency network by interfering with the signaling pathways that are inhibited in 2i conditions. To test this hypothesis, we analyzed the output of four pluripotency-associated signal transduction pathways in Pgk XX and E14 XY mESCs, including the MAPK/Mek and Gsk3 pathways, which are inhibited in 2i. We first identified target genes for Mek, Gsk3, Akt, and Stat3 from published microarray analyses of mESCs treated with pathway inhibitors and mutant cell lines (see Supplemental Experimental Procedures). We then analyzed the expression of these genes in our microarray data of undifferentiated cells grown in 2i medium (Figure 2C, open boxes) and in published RNA sequencing (RNA-seq) data (Marks et al., 2012), where the same cell lines had been analyzed in serum culture (Figure 2C, filled boxes). In 2i culture, target gene expression was only slightly affected by X dosage, but in serum, Mek and Gsk3 targets were reduced in

(E) Expression kinetics of genes with a strong delay in XX compared with XO and XY cells measured by microarray. The delay score for each gene is indicated below the gene name.
(F) Expression kinetics of the genes shown in Figure 1E were assessed in another XX/XO cell line pair (1.8XX/XO), maintained in serum-based medium and differentiated by LIF withdrawal. The mean and SD of three independent experiments are shown. *p < 0.05, two-sample Student's t test.
See also and Figure S1 and Tables S1, S2, and S3.

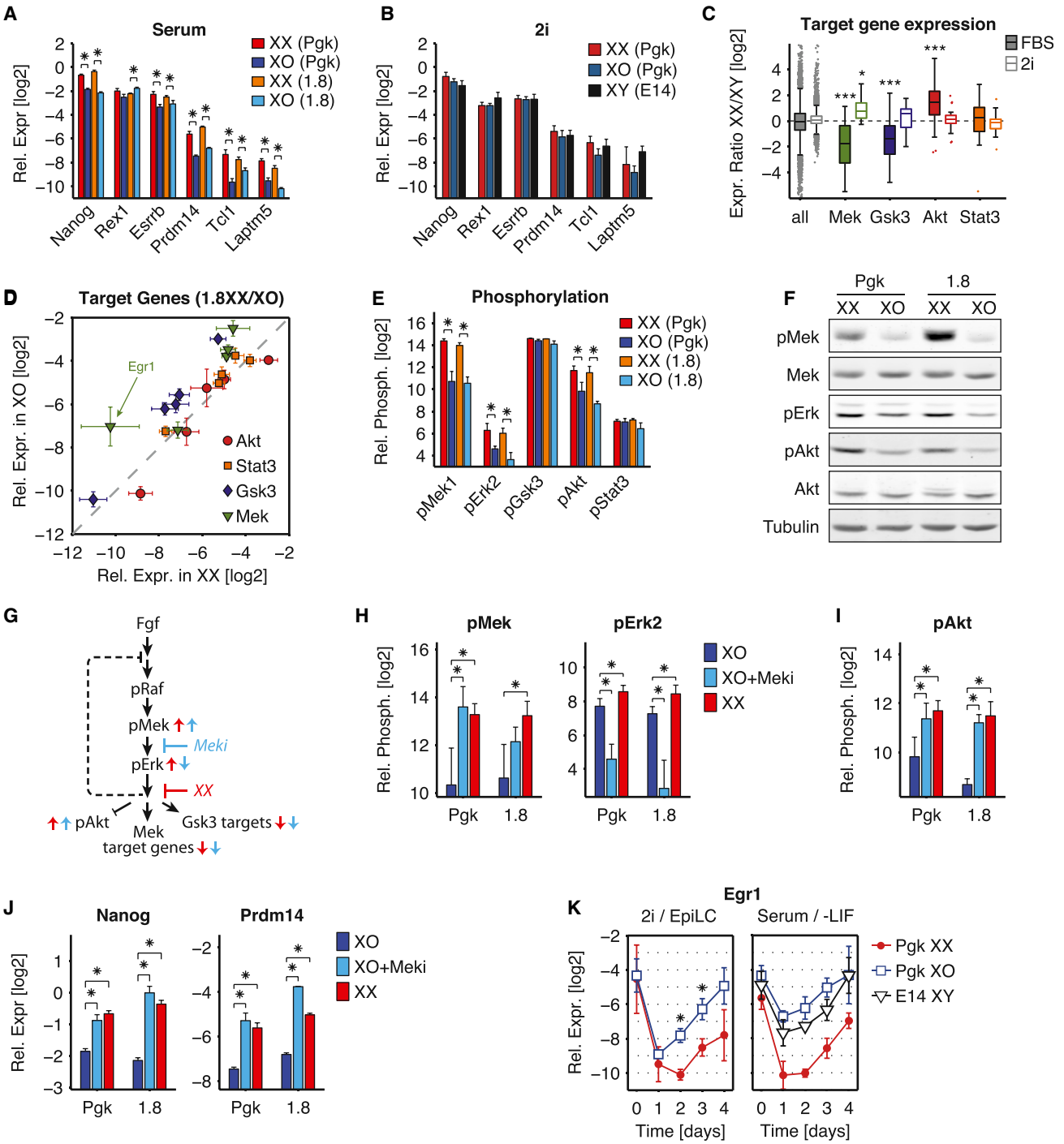

Figure 2. X Dosage Modulates Signaling Pathways in XX mESCs

(A and B) qPCR quantification of selected pluripotency-associated genes in two different XX/XO cell line pairs (Pgk12.1, 1.8) grown in serum-based medium (A) and in Pgk XX, XO, and E14 XY mESCs maintained in 2i medium (B).

(C) Target genes of the Mek, Gsk3, Akt, and Stat3 pathways were identified based on published genome-wide expression analyses upon inhibitor treatments. The expression ratio of Pgk XX versus E14 XY mESCs grown in 2i medium (open boxes) or serum (filled boxes; RNA-seq data from Marks et al., 2012) is shown. Boxes indicate the 25th to 75th percentiles and the central bar represents the median. *$p < 0.01$ and ***$p < 0.0001$, Wilcoxon rank-sum test.

(D) Five target genes for each pathway shown in (C) were assessed by qPCR in 1.8 XX and XO mESCs grown in serum-containing ESC medium. The mean and SD of nine independent experiments are shown.

(E and F) Phosphorylation levels of Mek, Erk2, Gsk3, Akt, and Stat3 were assessed in XX and XO mESC using Luminex technology (E), and differences were confirmed by immunoblotting (F).

(G) Schematic description of how Mek inhibition and X dosage affect the MAPK, Gsk3, and Akt pathways.

(legend continued on next page)

XX mESCs 3.3- and 2.6-fold, respectively, whereas Akt targets were increased 2.7-fold ($p < 10^{-4}$, Wilcoxon rank-sum test; Figure 2C). These X-dosage-dependent effects on target gene expression were confirmed in RNA-seq data for another XX/XY cell line pair (A.-V. Gendrel, M. Attia, C.-J. Chen, and N.B., unpublished data) and by quantitative PCR (qPCR) analysis of five target genes for each pathway in 1.8XX/XO and PgkXX/XO mESCs, which also exhibited the same trends (Figures 2D and S2B). We therefore conclude that X dosage inhibits Mek and Gsk3 signaling, but stimulates the Akt pathway.

To further investigate how X dosage affects signal transduction, we analyzed the phosphorylation levels of several pathway components in two XX/XO cell line pairs grown in serum, using Luminex bead assays (Figure 2E). No significant difference was observed for Gsk3 and Stat3 phosphorylation, but pMek and pErk, which are part of the MAPK pathway, as well as pAkt were increased 2- to 4-fold in XX mESCs (Figure 2E). The differences in phosphorylation levels of Mek, Erk, and Akt were also confirmed by immunoblotting (Figure 2F). Although elevated Akt phosphorylation in XX mESCs is consistent with the X-dosage-dependent increase of Akt target gene expression (Figure 2C), the increase in Mek and Erk phosphorylation was unexpected given that the MAPK pathway appeared to be inhibited by X dosage based on the target gene analysis (Figure 2C). However, such an increase in Mek phosphorylation when the MAPK pathway is inhibited has been observed previously (Fritsche-Guenther et al., 2011; Sturm et al., 2010) and is due to a reduction of negative feedback regulation, such that proteins that are upstream in the cascade are deactivated, which then dampens Mek phosphorylation (see scheme in Figure 2G). To confirm that this feedback is also operating in mESCs, we treated XO cells with a Mek inhibitor for 2 days. This treatment strongly increased Mek phosphorylation to levels comparable to those observed for XX ESCs (Figure 2H). As expected, phosphorylation of Erk, which lies downstream of Mek, was decreased upon inhibitor treatment (Figure 2H). The fact that X dosage, by contrast, increases Erk phosphorylation suggests that the inhibition of the MAPK pathway in XX mESCs occurs downstream of Erk (see scheme in Figure 2G).

The X-dosage-dependent modulation of Mek, Gsk3, and Akt target genes could be caused by distinct X-linked loci and/or arise from signaling crosstalk. In support of the latter possibility, we found that Mek inhibition increased Akt phosphorylation (Figure 2I). Moreover, Mek inhibition decreased three out of five Gsk3 targets tested, whereas inhibition of Gsk3 in turn had no detectable impact on Mek target genes (Figures S2C and S2D). Thus, signaling crosstalk whereby the MAPK pathway inhibits Akt signaling and promotes Gsk3 target gene expression might contribute to the variety of X-dosage-dependent effects on the mESC signaling network we observe. We therefore propose that one or more X-linked genes interfere with the MAPK signaling pathway and possibly also the Gsk3 and Akt pathways, thereby promoting the expression of pluripotency factors and thus stabilizing the pluripotent state directly and indirectly via signaling crosstalk. Consistent with this, Mek inhibition in XO mESCs was sufficient to increase Prdm14 and Nanog expression to the levels found in XX mESCs (Figure 2J). Although the X-dosage effect was neutralized by Mek and Gsk3 inhibition (in 2i), it again became effective once the inhibition was removed at the onset of differentiation, as judged by the mRNA levels of the MAPK target gene *Egr1* in differentiating XX and XO ESCs (Figures 2K and S3A). We thus propose that inhibition of MAPK signaling by X dosage, potentially together with additional mechanisms, is responsible for the delayed differentiation of XX mESCs described above.

Having uncovered an X-dosage-dependent inhibition of the MAPK pathway in the ESC tissue culture system, we tested whether two active X chromosomes have similar effects in embryos in vivo. The two X chromosomes in female embryos are both active for only a short time window of development, around embryonic day 4.5 (E4.5), shortly after imprinted XCI has been reversed (Mak et al., 2004; Okamoto et al., 2004). We thus performed single-cell qRT-PCR on E4.5 ICM cells isolated by immunosurgery (Figure S3B). Female epiblast cells, which have two active X chromosomes, showed a tendency to express lower levels of the MAPK target gene *Egr1* compared with their male counterparts, whereas Nanog levels appeared to be increased (Figure S3C). Given the technical challenge of analyzing large numbers of rather fragile epiblast cells, as well as the substantial variability between embryos and between cells, these differences were barely statistically significant (Figure S3C). In summary, we cannot conclude definitively that double X dosage inhibits MAPK signaling also in vivo, but the tendency seems to be the same as in ESCs.

X-Dosage-Dependent MAPK Inhibition Contributes to DNA Hypomethylation by Reducing Expression of Dnmt3a/b

In the next step, we investigated a potential link between X dosage and chromatin modifications, since global DNA methylation and histone acetylation at X-linked genes have been reported to respond to X dosage (O'Neill et al., 2003; Zvetkova et al., 2005). Although no major differences could be detected for histone methylation marks (Figure S4A), DNA methylation levels differed by 40%–50% between XX and XO/XY mESCs (Figure S4B). The latter finding is consistent with previous studies that reported global DNA hypomethylation in XX mESCs, possibly due to decreased expression of the de novo methyltransferases Dnmt3a and Dnmt3b (Habibi et al., 2013; Ooi et al., 2010; Zvetkova et al., 2005). To understand how X dosage affects DNA methylation, we analyzed the mRNA expression of seven genes involved in the regulation of DNA methylation, the DNA methyltransferases Dnmt1 and Dnmt3a/3b/3l, as well as three Tet enzyme genes, which are involved in DNA demethylation (Smith and Meissner, 2013). Two different XX/XO cell line pairs, maintained in serum-containing medium, exhibited an

(H–J) Mek inhibition (light blue) for 2 days with PD0325901 (1 μM) increases pMek, pAkt, Nanog, and Prdm14 levels in Pgk XO mESCs to the levels found in XX mESCs, but reduces pErk.

(K) Kinetics of the MAPK target gene *Egr1* during differentiation of XX, XO, and XY mESCs using two different culture/differentiation protocols (EpiLC and LIF withdrawal).

The mean and SD of three to five independent experiments are shown in (E) and (H)–(K); *$p < 0.05$, two-sample Student's t test. See also Figure S2.

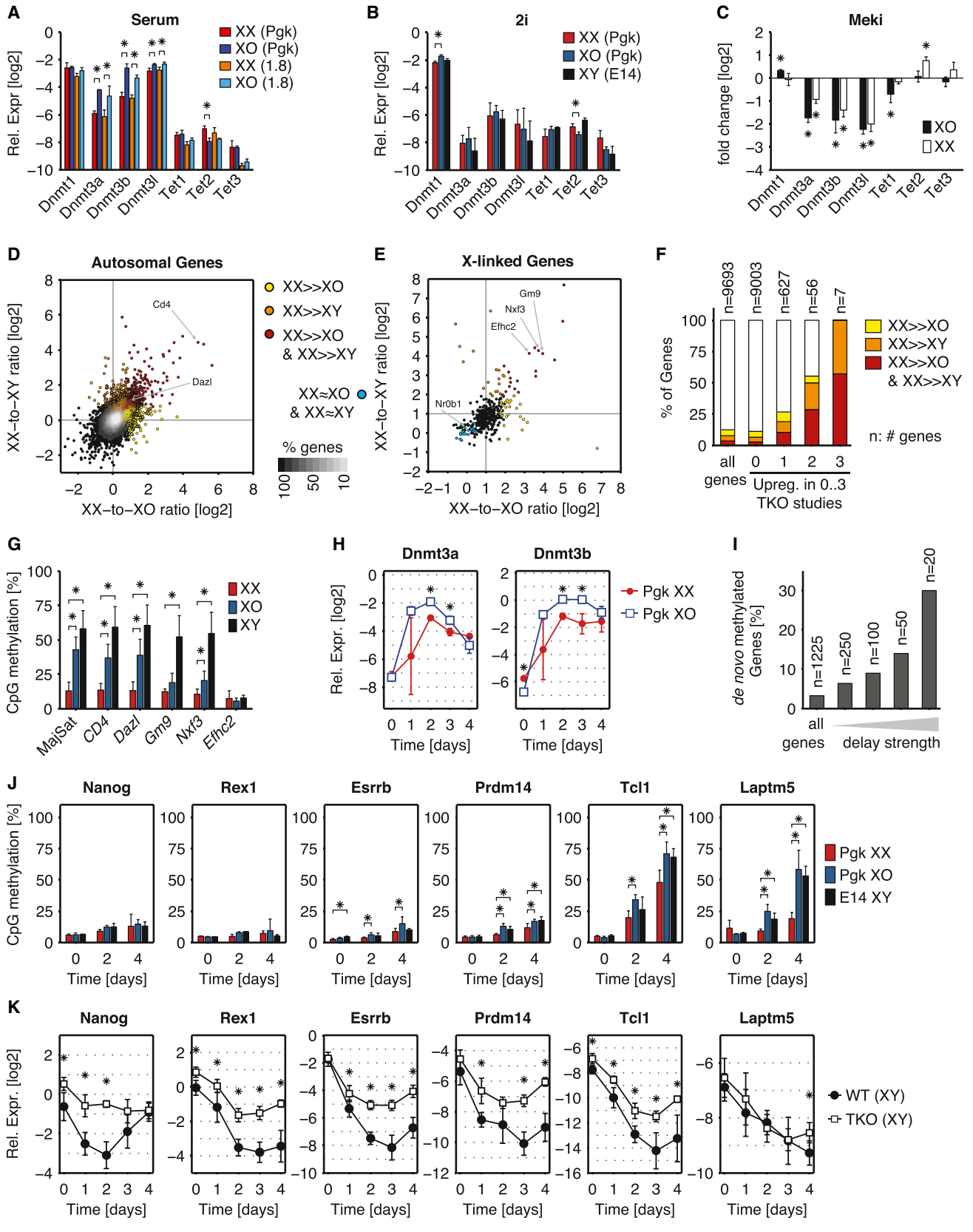

(legend on next page)

approximately 4-fold reduced expression of Dnmt3a and Dnmt3b in XX mESCs, a slight reduction in Dnmt3l expression, and a small increase in Tet2 expression (Figure 3A). X dosage therefore mainly reduced the expression of de novo methyltransferases Dnmt3a/b, as shown previously (Zvetkova et al., 2005), and seems to act at the transcriptional level. Since these XX/XO differences were only visible in serum culture and had disappeared after three to five passages in 2i medium (Figure 3B), we next tested whether de novo methyltransferases might be regulated by the MAPK pathway. Mek inhibition reduced expression of Dnmt3a, Dnmt3b, and Dnmt3l consistently in both Pgk XX and XO mESCs maintained in serum (Figure 3C). We therefore propose that MAPK inhibition in XX mESCs leads to a reduction of de novo methyltransferases and thereby contributes to the known DNA hypomethylation of XX cells. However, additional mechanisms are likely to be involved, since a recent genome-wide methylation analysis showed that even in 2i medium, female ESC lines maintain lower levels of DNA methylation compared with male lines (Habibi et al., 2013).

To understand whether DNA hypomethylation also affects transcription in an X-dosage-dependent manner, we analyzed the transcriptome data we had obtained for undifferentiated XX, XO, and XY mESCs (Figure 1A). The XX-to-XO and XX-to-XY expression ratios for the vast majority of autosomal genes were around 1 (0 in $\log_2$ scale), but a fraction of X-dosage-sensitive genes (322 out of 9,338; 3.4%) were expressed at higher levels in XX mESCs (Figure 3D). These autosomally encoded X-dosage-sensitive genes were candidates for potential derepression by DNA hypomethylation, as described below. On the X chromosome, the overwhelming majority of genes showed, as expected, a 2-fold higher expression in XX mESCs (1 in $\log_2$ scale; Figure 3E). Only a small number of X-linked genes (~20 out of 355; 5.6%), such as the pluripotency factor *Nr0b1/Dax1*, were expressed at similar levels in all three cell lines and thus seemed to be already dosage compensated in undifferentiated mESCs, possibly through gene-specific mechanisms (Figure 3E, blue). In addition, a group of genes on the X chromosome (19 out of 355; 5.4%) appeared to respond to X dosage even more strongly than expected (>2-fold increase in XX mESCs; Figure 3E; Table S4). To investigate whether the X-dosage-sensitive genes we identified on autosomes and on the X chromosome are derepressed in XX mESCs due to DNA hypomethylation of their promoters, we asked whether these genes respond to global loss of DNA methylation. For this purpose, we used transcriptome data from previously published studies that identified DNA methylation-sensitive genes in mESCs using a DNA methylation-deficient male Dnmt triple-knockout (TKO) ESC line (*Dnmt1*$^{-/-}$*Dnmt3a*$^{-/-}$*Dnmt3b*$^{-/-}$) (Tsumura et al., 2006). We saw that high-confidence DNA methylation-sensitive genes (identified in at least two studies) were highly enriched for X-dosage-sensitive genes (Fisher's exact test, $p < 10^{-18}$; Figure 3F). This finding was confirmed by the fact that four out of five of the derepressed genes tested showed lower DNA methylation levels at their promoters in XX (Pgk12.1) compared with XO (Pgk12.1-E8) and XY (E14) mESCs (Figure 3G). These findings are therefore consistent with the possibility that DNA hypomethylation results in derepression of some genes in female mESCs.

Because the transcriptome and methylation analyses described above (Figures 3D–3G) were performed after three to five passages in 2i conditions, which strongly impact global DNA methylation levels (Ficz et al., 2013; Habibi et al., 2013; Leitch et al., 2013), we investigated the dynamics of the serum-to-2i transition. Upon transfer to 2i medium, Dnmt3a/b levels were reduced and became indistinguishable in XX and XO mESCs after three to five passages (Figure S4C). Promoter methylation was progressively lost over eight passages (Figure S4D) and the associated genes (*Gm9*, *Nxf3*, *Dazl*, and *Cd4*) became derepressed (Figure S4E). Since methylation loss occurred with slower kinetics than Dnmt3a/b downregulation, XX mESCs still exhibited DNA hypomethylation after three to five passages in 2i (Figure 3G), although Dnmt3a/b were already expressed at similar levels in XX and XO cells (Figure 3B). Even after prolonged culture in 2i, when promoter methylation is completely lost, all X-dosage-sensitive genes tested showed higher transcript abundance in XX than in XO mESCs

Figure 3. DNA Methylation-Mediated Effects of MAPK Inhibition in XX mESCs

(A and B) Expression of DNA methylation regulators in two different XX/XO cell line pairs (Pgk12.1, 1.8) in serum-based medium (A) and in XX, XO, and XY ESCs maintained in 2i culture conditions (B).

(C) Response of methylation regulators to Mek inhibition (1 μM PD0325901) for 2 days in serum-based medium in PgkXX or XO mESCs.

(D and E) Transcriptome comparison of undifferentiated XX, XO, and XY mESCs. For all expressed autosomal (D) and X-linked genes (E), the XX/XO and XX/XY ratios are plotted. Gray lines indicate the expected ratios of 0 and 1, respectively. Genes with expression ratios significantly higher than expected are colored in yellow, red, and orange. Blue indicates the regime in which XX-to-XO/XY ratios are 0 and X-linked genes might already be dosage compensated. Genes that are analyzed in (G) are labeled with arrows. The number of genes in each category is given in Table S4.

(F) Genes that become derepressed upon loss of DNA methylation are enriched for X-dosage-sensitive genes. DNA methylation-sensitive genes were grouped into four categories depending on whether they were found to be upregulated in Dnmt-TKO mESCs in zero, one, two, or three different studies. The fractions of X-dosage-sensitive genes (red) and genes with an increased XX/XO or XX/XY ratio (yellow, orange) were calculated in each group. The number of genes in each category (n) is indicated above each bar.

(G) DNA methylation measured by mass-spectrometry-based EpiTyper analysis in XX, XO, and XY ESCs adapted to 2i culture conditions for three to five passages. Levels were assessed at major satellite repeat sequences as well as at the promoters of selected dosage-sensitive genes (indicated in D and E). The average fraction of methylated CpGs within the analyzed region is plotted.

(H) Expression of Dnmt3a and Dnmt3b as assessed by qPCR during EpiLC differentiation of Pgk XX/XO mESCs that had been adapted to 2i conditions for more than ten passages.

(I) Delayed genes (as in Figure 1C) were selected with different stringency and for each group the fraction of genes that gain methylation at their promoters during differentiation of ESCs into neural precursor cells is plotted.

(J) DNA methylation was measured by mass-spectrometry-based EpiTyper analysis or by Pyrosequencing at promoters of selected delayed genes at several time points during differentiation.

(K) Dnmt TKO cells and the parental J1 cell line were differentiated by LIF withdrawal, and the expression dynamics of selected genes were measured by qPCR. The mean and SD of three to six independent experiments are shown; *$p < 0.05$ in two-sample Student's t test. See also Figure S4 and Table S4.

(Figure S4E), suggesting that Dnmt3a/b-independent mechanisms must also contribute to gene derepression in XX mESCs. In summary, we propose that MAPK inhibition in XX mESCs is responsible for the reduced expression of de novo methyltransferases, which in turn is associated with DNA hypomethylation. Together with additional, as yet unidentified pathways, this mechanism might lead to the derepression of DNA methylation-sensitive genes that we observe in XX mESCs.

Double X Dosage Delays De Novo DNA Methylation during Differentiation

We next analyzed the possible role of X dosage in de novo DNA methylation during differentiation. As transcript levels of Dnmt3a/b are also decreased in XX compared with XO mESCs during differentiation (Figures 3H and S4F), reduced de novo methylation of pluripotency-associated genes might contribute to their delayed downregulation in XX mESCs. To investigate this hypothesis, we first assessed whether the genes that are up- or downregulated with a delay in XX cells are normally subject to promoter methylation during mESC differentiation. For this purpose, we compared our data with data from a previous study in which genome-wide DNA methylation profiles of mESCs and differentiated neural precursor cells were generated (Stadler et al., 2011). We found that up to 30% of the genes that were most delayed in differentiating XX mESCs gained de novo methylation at their promoters during mESC differentiation, compared with only 3% of all the genes that were up- or downregulated (GSEA, $p < 10^{-3}$; Figure 3I). For six strongly delayed genes, we also investigated whether, and to what extent, their promoters would gain methylation during early differentiation. Four genes (*Esrrb*, *Prdm14*, *Tcl1*, and *Laptm5*) showed lower methylation levels in XX cells during differentiation, albeit to a variable extent.

Based on these observations, we hypothesized that if impaired de novo methylation of stem cell genes contributes to the delayed differentiation of female cells, a DNA methylation-deficient male mESC line should also display delayed differentiation kinetics compared with its wild-type counterpart. Indeed, our analysis of the male Dnmt TKO mESC line (Tsumura et al., 2006) revealed that five out of six delayed genes analyzed were downregulated with slower kinetics in the Dnmt TKO mutant compared with the wild-type male parental mESC line (Figures 3K and S4G). As described in the original study by Tsumura et al. (2006), increased cell death was visible during differentiation of Dnmt TKO mESCs from day 3 onward, but the defect in downregulation of pluripotency factors was already detectable by days 1 and 2. Taken together, these findings show that, at least for a subset of genes, their delayed downregulation in XX cells is accompanied by a small delay in the appearance of de novo methylation at their promoters. Given that in male mESCs defective for de novo methylation the downregulation of pluripotency factors is also impaired, we propose that the delay in XX ESCs is partly due to reduced expression of de novo methyltransferases resulting from MAPK inhibition by double X dosage.

Ectopic XCI Can Reverse X-Dosage-Dependent MAPK Inhibition

If indeed a double dose of X-linked genes interferes with differentiation of XX mESCs through inhibition of MAPK signaling and reduction of DNA methylation, dosage compensation through X inactivation should neutralize the resulting sex differences. Consistent with this, DNA hypomethylation starts to disappear during ESC differentiation, when XCI is initiated (Figure S4H) and methylation levels as well as expression of pluripotency-associated genes become indistinguishable between male and female epiblast stem cell lines, which are derived from E6.5 embryos that have already completed XCI (Figure S4I; Guo et al., 2009). To test whether the increased expression of pluripotency factors, MAPK inhibition, and DNA hypomethylation that we observed in XX mESCs are indeed due to double X dosage, we used a system that allows ectopic induction of X inactivation by doxycyline treatment due to insertion of a tetracycline-inducible promoter at the transcriptional start site of the endogenous *Xist* gene. Previously, this system had only been used in male ESCs and in embryos (Savarese et al., 2006; Wutz et al., 2002). We derived a female mESC line heterozygous for the doxycycline-inducible promoter (TX1072; Figure 4A; see Experimental Procedures). Upon doxycycline treatment, an Xist-coated chromosome could be detected in ~70% of cells and X-linked genes were progressively silenced over several days (Figures 4B–4D). Interestingly, Xist induction appeared to increase cell proliferation of XX mESCs (E.G.S., unpublished observations). The phosphorylation levels of Mek were already strongly reduced after 2 days of induction and resembled the levels found in an XO control cell line (Figure 4E). Furthermore, Akt phosphorylation approached the reduced levels of the XO control. Only in the case of pErk was no significant change observed, presumably due to the small XX/XO difference in Erk phosphorylation in this particular cell line pair and to the low abundance of pErk in mESCs (Figure 4E). Global DNA methylation levels also exhibited a rather small difference of ~10% in the TX XX/XO cell line pair (Figure 4F). Nevertheless, methylation levels in XX cells became indistinguishable from the XO control upon doxycycline treatment, which was consistent with an increase in Dnmt3a/b expression (Figures 4F and 4G). Similarly, the subset of pluripotency-associated genes tested that exhibited a >2-fold XX/XO difference (*Nanog*, *Prdm14*, and *Tcl1*) was significantly decreased after 4–6 days of Xist induction (Figure 4G). Taken together, these findings strongly suggest that it is indeed a double dose of X-linked genes that stabilizes the pluripotent state and promotes DNA hypomethylation through modulation of signaling pathways in XX mESCs, and that the induction of XCI can overcome these effects, rendering XX ESCs similar to their XO or XY counterparts.

Pluripotency Factors and Xist RNA Show Reciprocal Expression in Single Cells

Next, we tested the hypothesis that during differentiation, XCI might overcome the XX-dependent differentiation arrest and facilitate the exit from the pluripotent state. This hypothesis predicts that cells that have undergone XCI will downregulate pluripotency factors. Taking advantage of the fact that not all XX cells undergo XCI during the time course analyzed (Figure S5A), we tested this hypothesis by single-cell qRT-PCR (Figure 5A). Using Xist expression to identify cells that had initiated XCI, we found that four out of six of the delayed genes tested (*Esrrb*, *Prdm14*, *Tcl1*, and *Laptm5*) were expressed

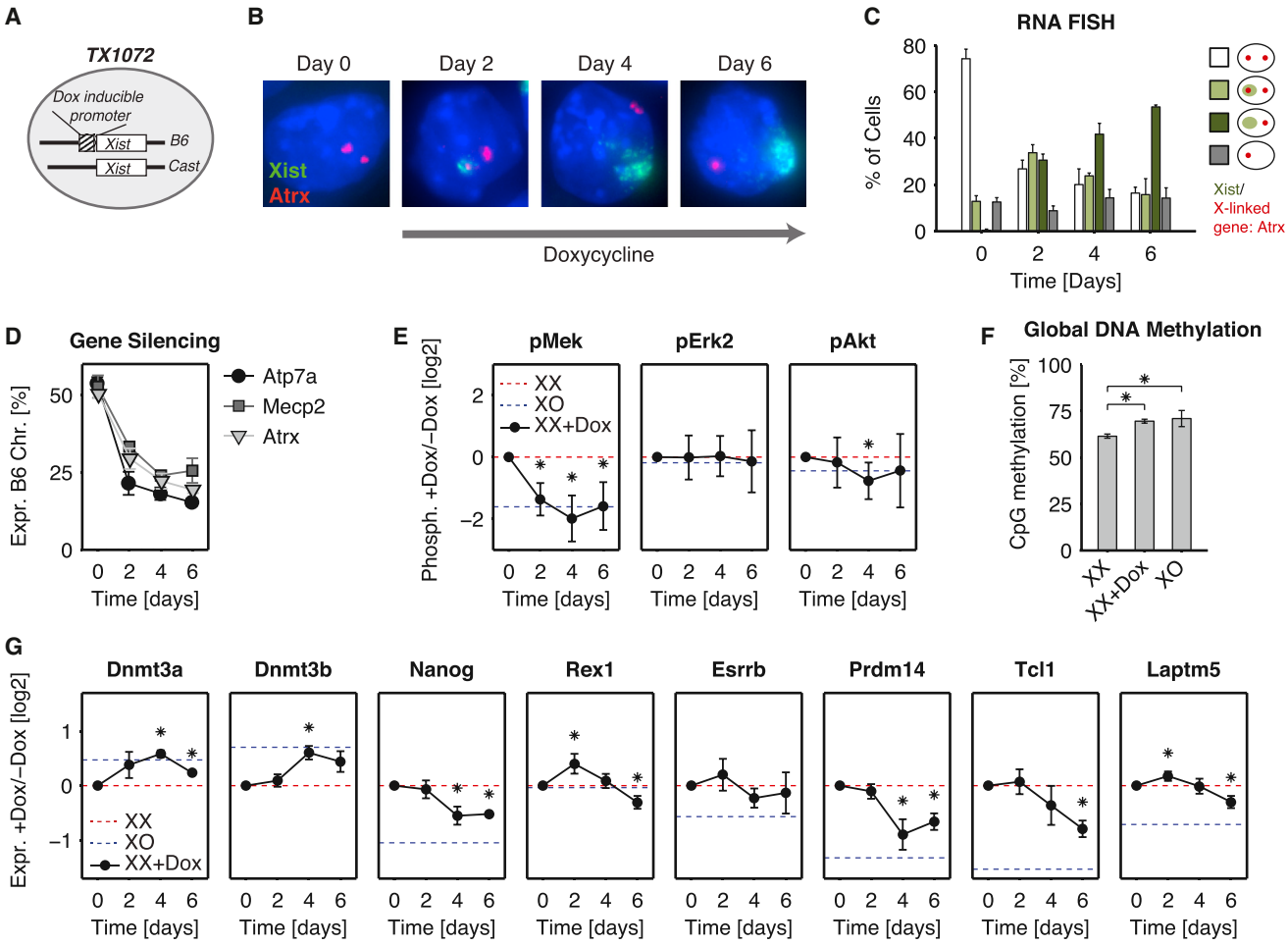

Figure 4. Forced X Inactivation Can Reverse X-Dosage Effects in Undifferentiated XX mESCs

(A) Schematic representation of the TX1072 cell line, in which Xist expression can be induced from the endogenous locus by doxycyline.

(B and C) Kinetics of Xist upregulation (green) and silencing of the X-linked *Atrx* gene (red) during doxycyline-dependent Xist induction in undifferentiated TX1072 mESCs as assessed by RNA FISH.

(D) Silencing of three X-linked genes upon Xist induction was assessed by Pyrosequencing.

(E) Mek, Erk, and Akt phosphorylation levels were measured by Luminex in the presence (black) and absence (red) of doxycyline and in TX1072 XO mESCs (blue dotted line). Phosphorylation was normalized to the levels in untreated XX cells (red).

(F) Global DNA methylation levels were assessed in TX1072 XX mESCs with and without 6 days of doxycyline treatment and in TX1072 XO cells using the Pyrosequencing-based Luminometeric DNA methylation assay (LUMA).

(G) Expression of selected genes was measured by qPCR in the presence (black) and absence (red) of doxycyline and in TX1072 XO mESCs (blue). Expression was normalized to the levels in untreated XX cells (red). The mean and SD of three to five independent experiments are shown; *$p < 0.05$ in paired Student's t test.

preferentially in Xist RNA-negative cells, while *Egr1* and *Dnmt3a/b* seemed to be expressed with higher probability in Xist RNA-positive cells (Figure 5B). These differences were more prominent at day 4 than at day 2 of differentiation, as expected given that X-linked gene silencing follows Xist RNA upregulation by a couple of days, being seen only after day 2 of differentiation (Chow et al., 2010). Although this finding is consistent with the idea that X inactivation facilitates differentiation, such a negative correlation between Xist RNA upregulation and pluripotency factor expression could also arise from the previously described repression of *Xist* by pluripotency factors (Augui et al., 2011; Navarro et al., 2008), whereby *Xist* would be upregulated preferentially after its repressors had been silenced.

X Inactivation Releases the Differentiation Arrest Exerted by Double X Dosage

In order to provide a direct demonstration that XCI promotes downregulation of pluripotency factors and thus releases the differentiation arrest in XX mESCs, we set out to perturb *Xist* expression in differentiating XX ESCs in two ways (Figure 5C). First, we used the TX1072 cell line described above, in which *Xist* upregulation can be induced ectopically, thereby uncoupling *Xist* expression from its endogenous regulators. Addition of doxycycline to the culture medium 1 day prior to the onset of differentiation resulted in accelerated *Xist* upregulation, as well as in an increased number of cells that underwent XCI (Figures 5D and S6A). During differentiation, four out of the six previously identified genes that are delayed in XX cells, in particular those

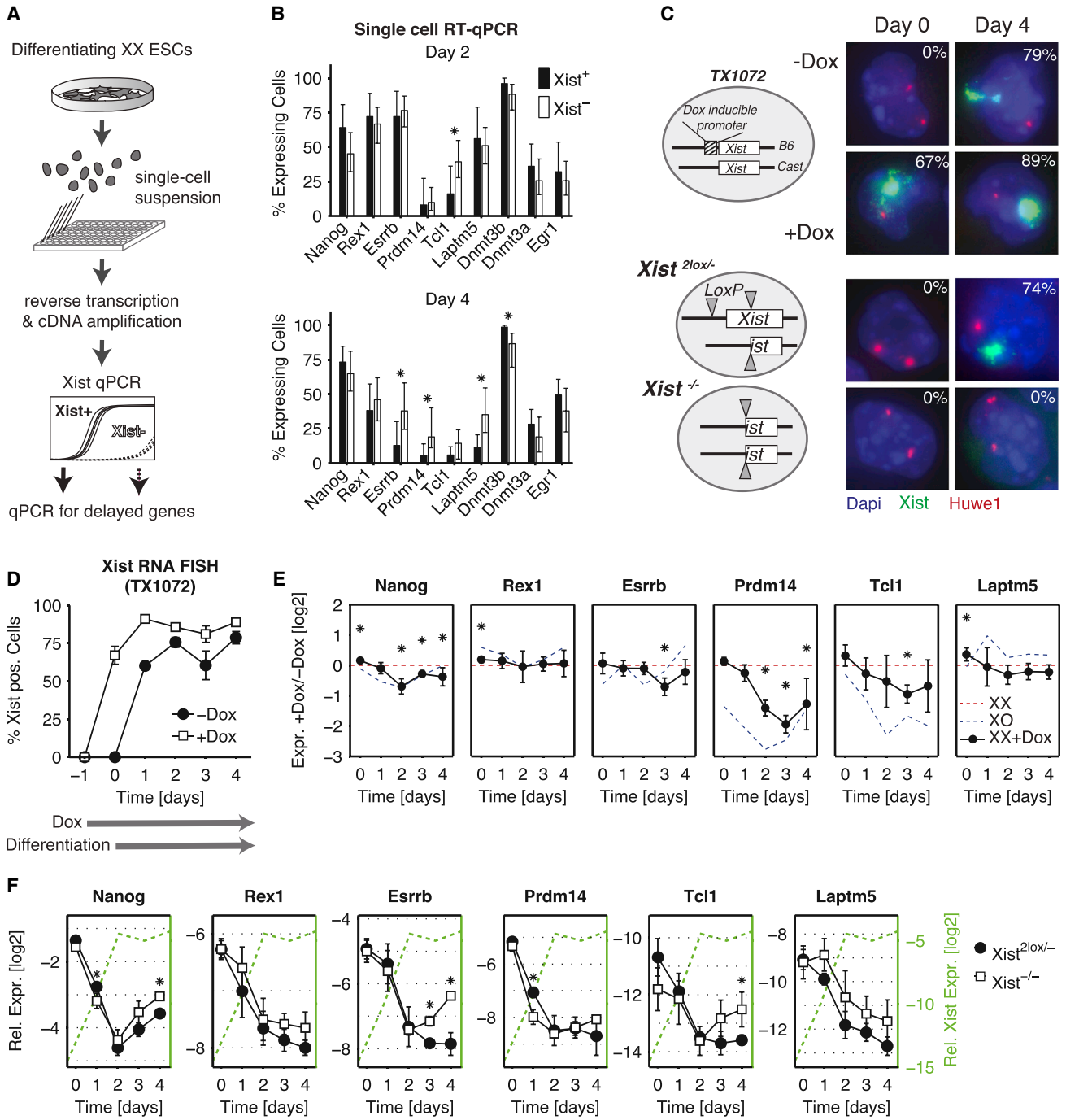

Figure 5. X Inactivation Releases the X-Dosage-Dependent Differentiation Block in XX ESCs

(A) Single-cell qRT-PCR protocol to assess expression patterns of delayed stem cell genes in Xist^{+} and Xist^{-} cells during differentiation of Pgk12.1 XX mESCs.

(B) Expression frequencies for selected genes in Xist^{+} and Xist^{-} cells are shown at day 2 (76 cells, top) and day 4 (108 cells, bottom) of differentiation (for more information, see Figure S5B). Error bars indicate the 95% confidence interval estimated by bootstrapping. *$p < 0.05$ in two-tailed Fisher's exact test.

(C) Approaches employed to perturb X inactivation kinetics: *Xist* deletion (bottom) and *Xist* upregulation prior to differentiation through a doxycycline-inducible promoter (TX1072). Xist upregulation was assessed by RNA FISH (green) together with the X-linked gene *Huwe1* (red) to confirm the presence of two X chromosomes in the cell. One representative cell is shown for each condition before (D0) and during (D4) differentiation.

(D) Xist expression in TX1072 cells differentiated in the presence (+Dox) or absence (−Dox) of doxycyline (added 1 day prior to differentiation), as assessed by Xist RNA FISH. The mean and SD of three independent experiments are shown; individual experiments are shown in Figure S6A.

(E) Expression of selected genes was measured by qPCR in the presence (black) and absence (red) of doxycyline and in a TX1072 XO line (blue). Expression was normalized to the levels in untreated XX cells (red).

(F) Differentiation kinetics of Xist$^{2lox/-}$ and Xist$^{-/-}$ mESCs. The kinetics of Xist upregulation in Xist$^{2lox/-}$ cells is indicated as a green dashed line.

The mean and SD of three to five independent experiments are shown; *$p < 0.05$ in paired (E) or two-sample (F) Student's t test. See also Figures S5 and S6.

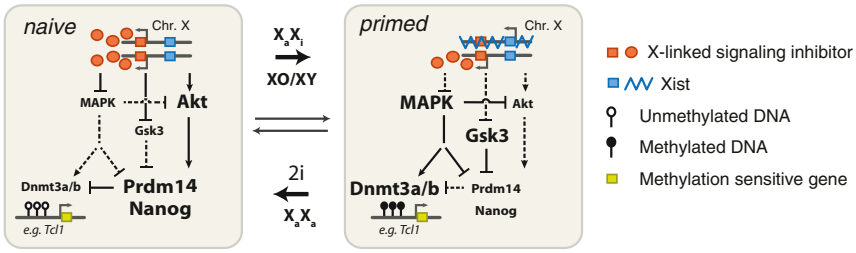

Figure 6. Model for How X Dosage Stabilizes the Pluripotent State and Blocks Differentiation

ESCs can fluctuate between the naive ground state of pluripotency (left) and a state primed for differentiation (right). One (or several) X-linked gene(s) (orange) present as a double dose in female XX ESCs interfere with the MAPK, Gsk3, and Akt signaling pathways, which in turn control pluripotency factors such as Nanog and Prdm14, and de novo DNA methyltransferases Dnmt3a/b. Consequently, X dosage stabilizes the pluripotent ground state and promotes DNA hypomethylation. Thus, female mESCs can only properly exit the pluripotent state after they have upregulated Xist (blue) and undergone X inactivation.

genes that showed a strong delay in the TX XX/XO cell line pair (*Nanog*, *Prdm14*, and *Tcl1*) were downregulated more strongly upon *Xist* induction by doxycycline treatment (Figure 5E), thereby demonstrating that experimentally accelerating X inactivation promotes a more rapid exit from the stem cell state in XX cells.

In the second approach, we set out to prevent *Xist* upregulation and XCI during female mESC differentiation. To this end, we generated a female mESC line in which *Xist* is deleted on both X chromosomes. We derived a female mESC line homozygous for the conditional $Xist^{2lox}$ allele (Csankovszki et al., 1999) and deleted *Xist*'s promoter together with its first three exons by Cre-mediated recombination. Whereas the heterozygous control line readily underwent XCI, $Xist^{-/-}$ cells failed to upregulate *Xist*, but nevertheless retained two X chromosomes in more than 80% of cells (Figures 5C, bottom, and S6B). During differentiation, $Xist^{-/-}$ cells maintained higher levels of three out of six of the delayed genes tested (*Nanog*, *Esrrb*, and *Tcl1*) compared with the heterozygous female control line (Figure 5F). These differences started to be visible around day 3 of differentiation, about 1 day after Xist had been upregulated in the control. In addition, Dnmt3a/b and Egr1 were expressed at lower levels in $Xist^{-/-}$ mESCs, presumably because these cells maintain a double dose of X-linked genes, which inhibit the MAPK pathway (Figure S6C).

Taken together, these findings support the hypothesis that XX status inhibits downregulation of pluripotency factors, and that once X chromosome dosage compensation is ensured, X inactivation feeds back into the pluripotency network and promotes differentiation.

DISCUSSION

The findings we present in this study demonstrate that double X dosage stabilizes the pluripotent state, and that female XX ESCs cannot complete differentiation until X inactivation has occurred. In the light of our data, we propose the following model for how X dosage affects stem cell maintenance and differentiation (Figure 6): Two active X chromosomes modulate the MAPK, Gsk3, and Akt signaling pathways, which regulate the pluripotent state. The resulting reduced MAPK activity in female ESCs shifts the population toward the naive ground state of pluripotency and thus increases the transcript levels of pluripotency factors. The reduced activity of MAPK signaling also results in DNA hypomethylation, which we propose participates in the slowed exit from the pluripotent state. However, DNA methylation-independent mechanisms are also likely to be involved. Consistent with this model, we demonstrate, using female ESCs that either accelerate or prevent XCI, that the presence of two active X chromosomes arrests differentiation of female mESCs until X inactivation has occurred and only a single dose of X-linked gene products remains. Until now, the coordination between X inactivation and development was thought to be ensured through repression of *Xist* by pluripotency factors, so that X inactivation would be initiated upon exit from the pluripotent state (Augui et al., 2011; Navarro et al., 2008). We show here, however, that X inactivation in turn also promotes differentiation, such that these two processes mutually regulate each other to ensure a tight coupling between X inactivation and development.

We show that X dosage affects three pathways that play important roles in the maintenance of pluripotency and in ESC differentiation: the MAPK/Erk, Gsk3, and Pi3K/Akt signaling pathways (Lanner and Rossant, 2010; Welham et al., 2011). Similar to the effects we observe in female mESCs, differentiation is blocked in cells and embryos deficient for Fgf-MAPK signaling or with constitutively activate Akt (Kunath et al., 2007; Lanner et al., 2009; Watanabe et al., 2006). Whether the different X-dosage-dependent effects are mediated by distinct X-linked loci or they arise from signaling crosstalk is still an open question. In principle, Lif signaling, which affects both the Pi3K/Akt and MAPK/Erk pathways could coordinate their activation (Niwa et al., 2009; Paling et al., 2004). However, this possibility seems unlikely since neither phosphorylation nor target gene expression of Stat3, the main mediator of Lif signaling, is affected by X dosage (Figures 2C–2E). Instead, we observed that Mek inhibition increases Akt phosphorylation (Figure 2I), such that MAPK inhibition could indirectly augment Akt target gene expression. Although the Akt and Gsk3 signaling pathways in turn could be coordinated by their common upstream kinase Pi3K (Welham et al., 2011), X dosage seems to interfere further downstream in the Gsk3 pathway, since phosphorylation of Gsk3 itself is not affected by X dosage. The role and mechanisms of crosstalk in mediating the various X-dosage-dependent effects we observe, as well as the implication of additional signaling-independent mechanisms, remain to be elucidated in the future.

Identifying the X-linked genes that are responsible for the stabilization of the pluripotent state that we have uncovered here will be challenging, since there are ~1,000 genes on the X chromosome, several of which might contribute to the observed effects. However, we can exclude the involvement of several known links between the X chromosome and pluripotency. The pluripotency factor Nr0b1/Dax1 is located on the X

chromosome, but it is not expressed in an X-dosage-sensitive manner, probably due to negative feedback regulation (Figure 3E). The X-linked E3 ubiquitin ligase Rlim/Rnf12, which promotes degradation of the pluripotency factor Zfp42/Rex1 (Gontan et al., 2012), can also be excluded because this link should rather destabilize the pluripotent state in XX ESCs. The inhibition of MAPK signaling that we describe here seems to be dominant over any potential pluripotency-destabilizing effect due to reduced Rex1 protein levels. Although Rex1 is widely used as a marker for pluripotent cells, its functional role in pluripotency and self-renewal is still debated (Kashyap et al., 2009). A well-known downstream effector of MAPK/Erk signaling, *Elk1*, is also located in the X. However, this should stimulate rather than inhibit MAPK signaling activity in XX ESCs. In human pluripotent stem cells (hPSCs), global effects on the transcriptome and on cell growth have been associated with the presence of two active X chromosomes and were attributed to increased Elk1 levels (Bruck et al., 2013). However, a parallel cannot be made with mESCs, as the latter require MAPK inhibition, whereas hPSCs depend on MAPK stimulation. We did test one potential inhibitor of MAPK signaling in XX mESCs, the X-linked Erk phosphatase Dusp9. However, knockdown and overexpression of Dusp9 had only a minor effect (data not shown). Another X-linked locus that could potentially be involved is the ESC-specific Pi3K activator Eras (Welham et al., 2011), but its contribution to increased Akt signaling in XX mESCs remains to be explored.

Recently, Prdm14 has been proposed to mediate the MAPK-dependent repression of Dnmt3a/b and to inhibit Fgf-MAPK signaling (Ficz et al., 2013; Grabole et al., 2013; Leitch et al., 2013; Yamaji et al., 2013). Since Prdm14 responds strongly to X dosage, it could in principle mediate the inhibition of MAPK signaling that we observe in female mESCs. However, Prdm14 inhibits Fgf-MAPK signaling by repressing the Fgf receptor 2 and thereby reduces Erk phosphorylation (Grabole et al., 2013; Yamaji et al., 2013), whereas we have shown that X dosage blocks the pathway downstream of Erk and increases pErk levels. Therefore, it is likely that upregulation of Prdm14 in XX mESCs is not the cause of X-dosage-dependent MAPK inhibition, but rather its consequence, since Prdm14 itself is a target of the pathway.

Are the drastic effects of X gene dosage that we observe in ESCs also expected to occur in vivo? Since a double dose of X-linked genes is only present for 1–2 days in the mouse embryo (Mak et al., 2004; Okamoto et al., 2004), X-dosage-dependent effects on pluripotency factors and DNA methylation might be less pronounced than in the mESC culture system. Thus, X dosage might only block differentiation in the rare cells that fail to initiate XCI efficiently, and might have a stronger impact only during the exit from diapause, a developmental arrest in the pluripotent ground state that occurs in mice if the mother is still lactating. Nevertheless, previous studies that compared the growth of embryos with XX and XO karyotypes reported in vivo effects of X dosage. XO embryos that carry a paternally derived X (X_pO) inactivate their single X during imprinted XCI, so that their development is retarded due to functional X nullosomy in extra-embryonic tissues (Jamieson et al., 1998; Thornhill and Burgoyne, 1993). The role of double X dosage can therefore only be assessed in the XX/X_mO comparison. Indeed, embryos with a single maternally derived X chromosome showed accelerated postimplantation development (Burgoyne et al., 1995; Thornhill and Burgoyne, 1993). A later paper reported no significant difference, but this was probably due to the low number of embryos analyzed (Jamieson et al., 1998). In light of our results, these observations raise the question as to how stabilization of the pluripotent state in female embryos might affect embryonic growth. Since transfer of ESCs into ground-state conditions (2i) generally tends to slow down proliferation (E.G.S., unpublished data), whereas ectopic XCI in XX mESCs appears to accelerate it, prolonged maintenance of the pluripotent state in female embryos might not only delay their development but also decrease their growth rate, thus resulting in a weight reduction of postimplantation embryos with two X chromosomes.

Although the presence of only a single X chromosome accelerates development, the persistence of double X dosage after implantation has detrimental consequences for the embryo and results in death at around E10 (Takagi and Abe, 1990). To prevent this, mechanisms have presumably evolved to ensure that all cells in a female embryo will undergo X inactivation. We propose that two active X chromosomes block differentiation in order to guarantee a tight coupling of X chromosome dosage and development. In differentiating male ESCs, ectopic *Xist* expression can initiate gene silencing only during a short time window in early differentiation (Wutz and Jaenisch, 2000). Through the X-dosage-dependent differentiation block that we have discussed here, this time window may be extended in female cells until X inactivation has occurred. A side effect of this "developmental checkpoint" would then be a small delay in the development of female embryos.

EXPERIMENTAL PROCEDURES

Detailed information on the cell lines used, culture and differentiation conditions, DNA methylation profiling, single-cell qRT-PCR on ESCs and E4.5 embryos, RNA fluorescence in situ hybridization (FISH), RNA extraction, reverse transcription, qPCR, microarray hybridization, and bioinformatic analyses are available in the Supplemental Experimental Procedures.

Bioinformatic Analyses

For analysis of the microarray time series, a subset of genes that show the strongest dynamics in expression within the XO and XX time series were defined (see Supplemental Experimental Procedures). To compare the XX, XO, and XY time series, the normalized Euclidean distance of the expression vectors at all time points in different cell lines was calculated after smoothing the time courses. To compute a score measuring delay, the set of regulated genes was further restricted to those genes that have a difference smaller than 1 in $\log_2$ expression in undifferentiated XO and XX ESCs. The delay score was computed by taking the average difference of the absolute numerical time derivative of the smoothed interpolated XO and XX time series.

GSEA was used to test for enrichment of gene sets with common GO biological process annotation (Subramanian et al., 2005). GSEA was also applied to test whether delayed genes gain de novo methylation during differentiation, using a set of de novo methylated genes, based on genome-wide methylation profiles of ESCs and differentiated neural precursor cells obtained by Stadler et al. (2011). Regions that were unmethylated (UMR) in mESCs and fully methylated (FMR) in neural precursor cells were defined as de novo methylated. If a 100 bp region (−50 to 50 bp) surrounding a gene's transcription start site overlaps with a de novo methylated region, the gene was defined as de novo methylated.

To define target gene signatures of pluripotency-associated signaling pathways, data from published studies in which specific pathways had been chemically or genetically inhibited (see Supplemental Experimental Procedures; Table S5 for details) were used. Briefly, for each data set, 150 genes with

the strongest fold change were identified and included in the pathway signature if they were found in the majority of experiments for a given pathway.

Single-Cell qRT-PCR

Single-cell qRT-PCR was performed essentially as described elsewhere (Tang et al., 2010).

Bio-Plex Assay

The level of phospho-protein expression was analyzed with the Bio-Plex Protein Array system (Bio-Rad) using a total protein amount of 15 μg per sample and multiplex assays consisting of the following analytes: p-Erk2 (Thr183/Tyr185), p-MEK1 (Ser217/Ser221), p-Akt (Ser473), p-Gsk3a/b (Ser21/Ser9), and p-Stat3 (Tyr705). The assay was performed according to the manufacturer's instructions, and beads and detection antibodies were further diluted three times.

ACCESSION NUMBERS

The large-scale data sets generated for this study have been deposited in the Gene Expression Omnibus database under accession number GSE44340.

SUPPLEMENTAL INFORMATION

Supplemental Information for this article includes Supplemental Experimental Procedures, six figures, and five tables and can be found with this article online at http://dx.doi.org/10.1016/j.stem.2013.11.022.

AUTHOR CONTRIBUTIONS

E.G.S. and E.H. conceived the study and wrote the paper. E.G.S. performed most of the experiments. C.P. and M.B. helped with ESC derivation, and A.S. performed the Bio-Plex assay. J.M. and N.B. performed the bioinformatic analyses, and I.O., T.N., and M.S. provided the in vivo data.

ACKNOWLEDGMENTS

We thank A. Wutz for the TX R26^{rtTA} mice, R. Jaenisch and J. Gribnau for the Xist^{2lox} mice, N. Brockdorff and T. Nesterova for Pgk12.1 and Pgk12.-E8(XO) mESC lines, M. Okano for Dnmt-TKO and J1 cell lines, A. Jouneau for male and female EpiSC lines, D. Schübeler for a list of regions that gain DNA methylation during ESC differentiation, and S. Keyse for the Dusp9 antibody. We thank the staff of the imaging facility PICTIBiSA@BDD for technical assistance, D. Gentien and C. Hego from the Institut Curie for microarray hybridizations, and M. Walter, J. Iranzo, and D. Bourc'his for help with the LUMA assay, embryo studies, and fruitful discussions. We thank K. Bernhard, F. S. Stewart, and A. Smith, who in the context of the EU FP7 SYBOSS (grant No. 242129) provided protocols and material for 2i culture and EpiLC differentiation. We are grateful to members of E.H.'s laboratory for critical input, and we thank E. Blackburn for a critical reading of the manuscript. This work was funded by an HFSP long-term fellowship (LT000597/2010-L) to E.G.S. and grants from the EU EpiGeneSys FP7 Network of Excellence No. 257082. N.B. was supported by BMBF (FORSYS).

Received: July 6, 2013
Revised: October 18, 2013
Accepted: November 26, 2013
Published: February 6, 2014

REFERENCES

Augui, S., Nora, E.P., and Heard, E. (2011). Regulation of X-chromosome inactivation by the X-inactivation centre. Nat. Rev. Genet. *12*, 429–442.

Bruck, T., Yanuka, O., and Benvenisty, N. (2013). Human pluripotent stem cells with distinct X inactivation status show molecular and cellular differences controlled by the X-linked ELK-1 gene. Cell Rep. *4*, 262–270.

Burgoyne, P.S., Thornhill, A.R., Boudrean, S.K., Darling, S.M., Bishop, C.E., and Evans, E.P. (1995). The genetic basis of XX-XY differences present before gonadal sex differentiation in the mouse. Philos. Trans. R. Soc. Lond. B Biol. Sci. *350*, 253–260, discussion 260–261.

Chow, J.C., Ciaudo, C., Fazzari, M.J., Mise, N., Servant, N., Glass, J.L., Attreed, M., Avner, P., Wutz, A., Barillot, E., et al. (2010). LINE-1 activity in facultative heterochromatin formation during X chromosome inactivation. Cell *141*, 956–969.

Csankovszki, G., Panning, B., Bates, B., Pehrson, J.R., and Jaenisch, R. (1999). Conditional deletion of Xist disrupts histone macroH2A localization but not maintenance of X inactivation. Nat. Genet. *22*, 323–324.

Ficz, G., Hore, T.A., Santos, F., Lee, H.J., Dean, W., Arand, J., Krueger, F., Oxley, D., Paul, Y.-L., Walter, J., et al. (2013). FGF signaling inhibition in ESCs drives rapid genome-wide demethylation to the epigenetic ground state of pluripotency. Cell Stem Cell *13*, 351–359.

Fritsche-Guenther, R., Witzel, F., Sieber, A., Herr, R., Schmidt, N., Braun, S., Brummer, T., Sers, C., and Blüthgen, N. (2011). Strong negative feedback from Erk to Raf confers robustness to MAPK signalling. Mol. Syst. Biol. *7*, 489.

Gontan, C., Achame, E.M., Demmers, J., Barakat, T.S., Rentmeester, E., van IJcken, W., Grootegoed, J.A., and Gribnau, J. (2012). RNF12 initiates X-chromosome inactivation by targeting REX1 for degradation. Nature *485*, 386–390.

Grabole, N., Tischler, J., Hackett, J.A., Kim, S., Tang, F., Leitch, H.G., Magnúsdóttir, E., and Surani, M.A. (2013). Prdm14 promotes germline fate and naive pluripotency by repressing FGF signalling and DNA methylation. EMBO Rep. *14*, 629–637.

Graf, T., and Stadtfeld, M. (2008). Heterogeneity of embryonic and adult stem cells. Cell Stem Cell *3*, 480–483.

Guo, G., Yang, J., Nichols, J., Hall, J.S., Eyres, I., Mansfield, W., and Smith, A. (2009). Klf4 reverts developmentally programmed restriction of ground state pluripotency. Development *136*, 1063–1069.

Habibi, E., Brinkman, A.B., Arand, J., Kroeze, L.I., Kerstens, H.H.D., Matarese, F., Lepikhov, K., Gut, M., Brun-Heath, I., Hubner, N.C., et al. (2013). Whole-genome bisulfite sequencing of two distinct interconvertible DNA methylomes of mouse embryonic stem cells. Cell Stem Cell *13*, 360–369.

Hayashi, K., Ohta, H., Kurimoto, K., Aramaki, S., and Saitou, M. (2011). Reconstitution of the mouse germ cell specification pathway in culture by pluripotent stem cells. Cell *146*, 519–532.

Jamieson, R.V., Tan, S.S., and Tam, P.P. (1998). Retarded postimplantation development of X0 mouse embryos: impact of the parental origin of the monosomic X chromosome. Dev. Biol. *201*, 13–25.

Kashyap, V., Rezende, N.C., Scotland, K.B., Shaffer, S.M., Persson, J.L., Gudas, L.J., and Mongan, N.P. (2009). Regulation of stem cell pluripotency and differentiation involves a mutual regulatory circuit of the NANOG, OCT4, and SOX2 pluripotency transcription factors with polycomb repressive complexes and stem cell microRNAs. Stem Cells Dev. *18*, 1093–1108.

Kunath, T., Saba-El-Leil, M.K., Almousailleakh, M., Wray, J., Meloche, S., and Smith, A. (2007). FGF stimulation of the Erk1/2 signalling cascade triggers transition of pluripotent embryonic stem cells from self-renewal to lineage commitment. Development *134*, 2895–2902.

Lanner, F., and Rossant, J. (2010). The role of FGF/Erk signaling in pluripotent cells. Development *137*, 3351–3360.

Lanner, F., Lee, K.L., Sohl, M., Holmborn, K., Yang, H., Wilbertz, J., Poellinger, L., Rossant, J., and Farnebo, F. (2009). Heparan sulfation-dependent fibroblast growth factor signaling maintains embryonic stem cells primed for differentiation in a heterogeneous state. Stem Cells *28*, 191–200.

Leitch, H.G., McEwen, K.R., Turp, A., Encheva, V., Carroll, T., Grabole, N., Mansfield, W., Nashun, B., Knezovich, J.G., Smith, A., et al. (2013). Naive pluripotency is associated with global DNA hypomethylation. Nat. Struct. Mol. Biol. *20*, 311–316.

Mak, W., Nesterova, T.B., de Napoles, M., Appanah, R., Yamanaka, S., Otte, A.P., and Brockdorff, N. (2004). Reactivation of the paternal X chromosome in early mouse embryos. Science *303*, 666–669.

Marks, H., Kalkan, T., Menafra, R., Denissov, S., Jones, K., Hofemeister, H., Nichols, J., Kranz, A., Stewart, A.F., Smith, A., and Stunnenberg, H.G. (2012). The transcriptional and epigenomic foundations of ground state pluripotency. Cell *149*, 590–604.

Mittwoch, U. (1993). Blastocysts prepare for the race to be male. Hum. Reprod. *8*, 1550–1555.

Navarro, P., Chambers, I., Karwacki-Neisius, V., Chureau, C., Morey, C., Rougeulle, C., and Avner, P. (2008). Molecular coupling of Xist regulation and pluripotency. Science *321*, 1693–1695.

Nichols, J., and Smith, A. (2009). Naive and primed pluripotent states. Cell Stem Cell *4*, 487–492.

Niwa, H., Ogawa, K., Shimosato, D., and Adachi, K. (2009). A parallel circuit of LIF signalling pathways maintains pluripotency of mouse ES cells. Nature *460*, 118–122.

O'Neill, L.P., Randall, T.E., Lavender, J., Spotswood, H.T., Lee, J.T., and Turner, B.M. (2003). X-linked genes in female embryonic stem cells carry an epigenetic mark prior to the onset of X inactivation. Hum. Mol. Genet. *12*, 1783–1790.

Okamoto, I., Otte, A.P., Allis, C.D., Reinberg, D., and Heard, E. (2004). Epigenetic dynamics of imprinted X inactivation during early mouse development. Science *303*, 644–649.

Ooi, S.K., Wolf, D., Hartung, O., Agarwal, S., Daley, G.Q., Goff, S.P., and Bestor, T.H. (2010). Dynamic instability of genomic methylation patterns in pluripotent stem cells. Epigenetics Chromatin *3*, 17.

Paling, N.R.D., Wheadon, H., Bone, H.K., and Welham, M.J. (2004). Regulation of embryonic stem cell self-renewal by phosphoinositide 3-kinase-dependent signaling. J. Biol. Chem. *279*, 48063–48070.

Savarese, F., Flahndorfer, K., Jaenisch, R., Busslinger, M., and Wutz, A. (2006). Hematopoietic precursor cells transiently reestablish permissiveness for X inactivation. Mol. Cell. Biol. *26*, 7167–7177.

Schulz, E.G., and Heard, E. (2013). Role and control of X chromosome dosage in mammalian development. Curr. Opin. Genet. Dev. *23*, 109–115.

Smith, Z.D., and Meissner, A. (2013). DNA methylation: roles in mammalian development. Nat. Rev. Genet. *14*, 204–220.

Stadler, M.B., Murr, R., Burger, L., Ivanek, R., Lienert, F., Schöler, A., van Nimwegen, E., Wirbelauer, C., Oakeley, E.J., Gaidatzis, D., et al. (2011). DNA-binding factors shape the mouse methylome at distal regulatory regions. Nature *480*, 490–495.

Sturm, O.E., Orton, R., Grindlay, J., Birtwistle, M., Vyshemirsky, V., Gilbert, D., Calder, M., Pitt, A., Kholodenko, B., and Kolch, W. (2010). The mammalian MAPK/ERK pathway exhibits properties of a negative feedback amplifier. Sci. Signal. *3*, ra90.

Subramanian, A., Tamayo, P., Mootha, V.K., Mukherjee, S., Ebert, B.L., Gillette, M.A., Paulovich, A., Pomeroy, S.L., Golub, T.R., Lander, E.S., and Mesirov, J.P. (2005). Gene set enrichment analysis: a knowledge-based approach for interpreting genome-wide expression profiles. Proc. Natl. Acad. Sci. USA *102*, 15545–15550.

Takagi, N., and Abe, K. (1990). Detrimental effects of two active X chromosomes on early mouse development. Development *109*, 189–201.

Tang, F., Barbacioru, C., Nordman, E., Li, B., Xu, N., Bashkirov, V.I., Lao, K., and Surani, M.A. (2010). RNA-Seq analysis to capture the transcriptome landscape of a single cell. Nat. Protoc. *5*, 516–535.

Thornhill, A.R., and Burgoyne, P.S. (1993). A paternally imprinted X chromosome retards the development of the early mouse embryo. Development *118*, 171–174.

Tsumura, A., Hayakawa, T., Kumaki, Y., Takebayashi, S.-I., Sakaue, M., Matsuoka, C., Shimotohno, K., Ishikawa, F., Li, E., Ueda, H.R., et al. (2006). Maintenance of self-renewal ability of mouse embryonic stem cells in the absence of DNA methyltransferases Dnmt1, Dnmt3a and Dnmt3b. Genes Cells *11*, 805–814.

Watanabe, S., Umehara, H., Murayama, K., Okabe, M., Kimura, T., and Nakano, T. (2006). Activation of Akt signaling is sufficient to maintain pluripotency in mouse and primate embryonic stem cells. Oncogene *25*, 2697–2707.

Welham, M.J., Kingham, E., Sanchez-Ripoll, Y., Kumpfmueller, B., Storm, M., and Bone, H. (2011). Controlling embryonic stem cell proliferation and pluripotency: the role of PI3K- and GSK-3-dependent signalling. Biochem. Soc. Trans. *39*, 674–678.

Wutz, A., and Jaenisch, R. (2000). A shift from reversible to irreversible X inactivation is triggered during ES cell differentiation. Mol. Cell *5*, 695–705.

Wutz, A., Rasmussen, T.P., and Jaenisch, R. (2002). Chromosomal silencing and localization are mediated by different domains of Xist RNA. Nat. Genet. *30*, 167–174.

Yamaji, M., Ueda, J., Hayashi, K., Ohta, H., Yabuta, Y., Kurimoto, K., Nakato, R., Yamada, Y., Shirahige, K., and Saitou, M. (2013). PRDM14 Ensures Naive Pluripotency through Dual Regulation of Signaling and Epigenetic Pathways in Mouse Embryonic Stem Cells. Cell Stem Cell *12*, 368–382.

Ying, Q.-L., Wray, J., Nichols, J., Batlle-Morera, L., Doble, B., Woodgett, J., Cohen, P., and Smith, A. (2008). The ground state of embryonic stem cell self-renewal. Nature *453*, 519–523.

Zvetkova, I., Apedaile, A., Ramsahoye, B., Mermoud, J.E., Crompton, L.A., John, R., Feil, R., and Brockdorff, N. (2005). Global hypomethylation of the genome in XX embryonic stem cells. Nat. Genet. *37*, 1274–1279.